
Article:
Otitoju, O., Oko, E. orcid.org/0000-0001-9221-680X and Wang, M. orcid.org/0000-0001-9752-270X (2020) A new method for scale-up of solvent-based post-combustion carbon capture process with packed columns. International Journal of Greenhouse Gas Control, 93. 102900. ISSN 1750-5836

https://doi.org/10.1016/j.ijggc.2019.102900

A new method for scale-up of solvent-based post-combustion carbon capture process with packed columns

Otitoju Olajide, Eni Oko, Meihong Wang*

Department of Chemical and Biological Engineering, The University of Sheffield, Sheffield S1 3JD, UK

*Corresponding author: E-mail address: Meihong.wang@sheffield.ac.uk, Tel: +44(0)114 – 2227–160

Abstract

Solvent-based post-combustion carbon capture (PCC) with packed column is the most commercially ready CO_2 capture technology. To study commercial-scale PCC processes, validated pilot scale models are often scaled up to commercial-scale using the generalized pressure drop correlation (GPDC) chart which requires assuming the column pressure drop. The GPDC method may lead to either over-estimation or under-estimation of the column diameter. In this paper, a new method for estimating the packed column diameter without assuming the pressure drop has been proposed and used for model scale-up. The method was validated by scaling between two existing pilot plant sizes. The CO_2 capture process was simulated in Aspen Plus® and validated at pilot scale. The validated model was scaled up to commercial CO_2 capture plant capable of serving a 250 MW_e combined cycle gas turbine power plant using the new method proposed in this study. The results obtained from the scale-up study were compared to those obtained when the GPDC method was used to design the same commercial CO_2 capture plant. The results showed that the GPDC method overestimated the absorber and stripper diameter by 1.6% and 8.5% respectively. Process simulation results for the commercial-scale plant showed about 2.12% and 5.63% lower solvent flow rate and reboiler duty with the proposed method. Therefore, the capital and operating costs for the process using the newly proposed scale-up method could be lower based on our estimates of the column dimensions, solvent flow rate and specific reboiler duty.

Keywords: post-combustion CO_2 capture, chemical absorption, process modelling and simulation, model validation, scale-up, combined cycle gas turbine power plant

Highlights

- Generalized pressure drop correlation (GPDC) commonly used for scale-up in carbon capture.
- New method to estimate packed column diameter proposed.

- Rate-based model developed and validated at pilot scale for MEA-based PCC in Aspen Plus® V8.4.
- New scale-up method validated using two existing pilot plants.
- Scale-up of MEA-based PCC process based on the proposed method carried out.

Nomenclature

a	specific surface area of packing (m^2/m^3)
C_i	concentration of component i. ($kmol/m^3$)
CP	capacity parameter
D	diameter (m)
E_j	activation energy (kJ/mol)
F_{LV}	flow parameter
F_p	packing factor (m^{-1})
G	gas mass flow rate (kg/s)
G_i	gas molar flow rate per cross-sectional area (kmol/m^2 s)
H_{OG}	height of the transfer unit (m)
K_G	overall gas-phase mass transfer coefficient (kmol/m^3 s bar)
k_j^o	pre-exponential factor ($m^3/kmol.s$)
L	solvent mass flow rate (kg/s)
M_{MEA}	molar mass of MEA (kg/kmol)
n	Temperature factor
N_{OG}	overall number of the transfer unit
P	pressure (bar)
ΔP_{fl}	flooding pressure drop (in.H_2O/ft)
R	ideal gas constant (J/K mol)
R_j	Reaction rate for reaction j, ($m^3/kmol.s$)
T	Temperature (K)
$V_{G,fl}$	flooding velocity (m/s)
V_G	superficial gas velocity (m/s)
y	mole fraction of CO_2 in the gas phase at any point in the column
$y_{CO_{2,in}}$	mole fraction of CO_2 in the inlet gas

$y_{CO_{2,out}}$ mole fraction of CO_2 in the outlet gas

y^* gas-phase mole fraction of CO_2 in equilibrium with CO_2 concentration in the liquid

z number of equivalents/moles of amine (1 for MEA)

Z_T packing height (m)

Greek letters

α_{Lean} lean loading (mol CO_2/mol MEA)

α_{Rich} rich loading (mol CO_2/mol MEA)

$\Delta\alpha$ absorption capacity (mol CO_2/mol MEA)

α_{ij} specie i reaction order in reaction j

ρ_G gas density (kg/m^3)

ρ_L liquid density (kg/m^3)

ε porosity

v kinematic viscosity (cst)

φ_{CO_2} percentage of CO_2 captured

ω_{MEA} MEA concentration (wt%)

Abbreviations

CCGT Combined Cycle Gas Turbine

GPDC Generalized pressure drop correlation

HETP Height Equivalent to the Theoretical Plate

PCC Post-Combustion Carbon Capture

PRE Percentage relative error

SRP Separation Research Programme

1. Introduction

1.1.Background

There is an increasing concern about global warming effect arising from the emission of greenhouse gases (GHGs). Anthropogenic CO_2 emissions from different sources constitute about 80% of the total GHG emissions (Sreedhar et al., 2017), and CO_2 emissions from fossil

fuel-fired power plants are responsible for approximately about 25% of the total GHG (Soltani et al., 2017; EPA, 2017).This indicates that efforts at reducing GHG emissions must be targeted at cutting down CO_2 emissions from these facilities. One way to achieve this is through the deployment of cost-effective CO_2 capture technologies in fossil fuel-fired power plants.

There are three technological options for CO_2 capture: pre-combustion, oxy-fuel combustion and post-combustion. Among these capture technologies, post-combustion CO_2 capture through chemical absorption with amines is the most mature technology to be used to cut down CO_2 emissions from power plants (Wang et al., 2011). In addition to this, the technology is considered the best option for retrofit as its implementation in an existing power plant requires very little modifications (Rezazadeh et al., 2017). Despite these advantages, the commercial implementation of the solvent-based PCC process is faced with a number of challenges such as high capital cost and high energy consumption.

1.2 Previous studies

Process modelling and simulation is critical to the design and operation of the PCC plant, and several studies with focus on model development for the plant have been carried out (Awoyomi et al., 2019; Bui et al., 2018; Enaasen et al., 2015; Garcia et al., 2017; Khan et al., 2011; Lawal et al., 2009; Soltani et al., 2017; Zhang et al., 2009). Earlier studies focussed on model development for the standalone absorber (Khan et al., 2011; Kvamsdal et al., 2009; Lawal et al., 2009; Zhang et al., 2009) and the standalone stripper (Greer et al., 2010; Ziaii et al., 2009). This was followed by model development for the whole solvent-based PCC plant (Gaspar and Cormos, 2012; Harun et al., 2012; Lawal et al., 2010; Warudkar et al., 2013; Zhang and Chen, 2013). The reliability of the models' predictions was validated using published experimental data collected from various pilot plants around the world. Experimental data to which model predictions are commonly compared in the literature are the CO_2 capture level (Errico et al., 2016; Harun et al., 2012; Lawal et al., 2009; Razi et al., 2013; Zhang et al., 2009), rich solvent CO_2 loading (Enaasen Flø et al., 2015; Khan et al., 2011; Luo and Wang, 2017), temperature profile (Bui et al., 2014; Canepa et al., 2013; Garcia et al., 2017; Khan et al., 2011; Lawal et al., 2009; Razi et al., 2013), CO_2 concentration profiles (Khan et al., 2011; Luo and Wang, 2017; Razi et al., 2013), desorbed CO_2 (Garcia et al., 2017) and specific heat duty (Agbonghae et al., 2014; Luo and Wang, 2017).

Zhang et al. (2009) validated the rate-based absorber model developed in Aspen Plus® with a pilot plant data by the Separations Research Programmes (SRP) at the University of Texas.

The model was validated against the following parameters: CO_2 capture level, CO_2 loadings, and temperature profiles. The model predictions showed excellent agreement with the pilot plant data for each of the parameters. Khan et al. (2011) validated their rate-based model with the pilot and industrial-scale experimental data collected from the studies of Pintola et al. (1993), Tontiwachwuthikul et al. (1992) and Aroonwilas et al. (2001). The model predictions matched experimental measurements for the liquid phase MEA and gas-phase CO_2 concentrations and the liquid phase temperature profiles.

In order to design and study the possible requirements of a commercial-scale MEA-based CO_2 capture process, the validated pilot-scale models are often scaled to commercial scale. Several researchers (Agbonghae et al., 2014; Awoyomi et al., 2019; Biliyok and Yeung, 2013; Canepa et al., 2013; Dutta et al., 2017; Lawal et al., 2012; Nittaya et al., 2014) have performed model scale-up of the process from pilot scale to commercial scale. Lawal et al. (2012) designed a commercial CO_2 capture plant that is capable of capturing 90% of CO_2 from the flue gas stream of a 500 MW_e subcritical coal-fired power plant by scaling-up the validated CO_2 capture pilot plant model developed in gPROMS. Using the generalized pressure drop correlation chart (GPDC), they developed a capture plant with two absorbers each of diameter 9 m and height 27 m and a stripper having the same diameter as the absorber. Similarly, Nittaya et al. (2014) scaled up the CO_2 capture pilot plant model developed in gPROMS to a commercial CO_2 capture plant capable of capturing 87% of CO_2 from the flue gas of a 700 MW_e supercritical coal-fired power plant. Their scale-up resulted in a commercial CO_2 capture plant with three absorbers, each with a diameter of 11.8 m and height of 34 m and two strippers each having a diameter of 10.4 m and height of 16 m. Agbonghae et al. (2014) scaled up a validated CO_2 capture pilot plant model developed in Aspen Plus® to a commercial CO_2 capture plant capable of capturing 90% of CO_2 from the flue gas of a 400 MW_e CCGT power plant. They came up with a CO_2 capture plant with two absorbers, each with a diameter of 11.93 m and height of 19.06 m and a stripper with a diameter of 6.76 m and height of 28.15 m. In all the studies above, the commercial-scale designs of the absorber and the stripper are based on the GDPC method—which involves assuming the column pressure drop. This study is focussed on developing an alternative method to estimate the diameter of the packed column for solvent-based PCC process using an empirical correlation that estimates the flooding gas velocity. This allows the diameter of the packed column to be calculated without assuming the pressure drop.

1.3 Aims and novelty of this study

Model scale-up from pilot scale to commercial scale for the solvent-based PCC will not only help in providing insights into plant operations but also foresee any commercial-scale development and operational bottlenecks. For the solvent-based PCC process, the packed bed absorber and the stripper are the two largest components in terms of size (Agbonghae et al., 2014; Lawal et al., 2012) and cost (Abu-Zahra et al., 2007). Their design as reported in the literature is based on chemical engineering principles using the GPDC method. Sinnott (2005) recommended a pressure drop range of 147 to 490 Pa/m of packing for packed column design at commercial scale. Within this pressure drop range, experimental data are only available at 206 and 412 Pa/m of packing on the GPDC chart thereby limiting the choice of pressure drop that can be assumed within this range. Furthermore, data interpolation for pressure drop are difficult and could lead to inaccurate estimates. In existing studies (Agbonghae et al., 2014; Awoyomi et al., 2019; Canepa et al., 2013; Dutta et al., 2017; Lawal et al., 2012; Luo and Wang, 2017; Nittaya et al., 2014), pressure drop of either 206 or 412 Pa/m of packing has been assumed. To address this limitation, this study aims to propose an alternative method to estimate the packed column diameter that does not require assuming the column pressure drop. The method involves an algebraic equation derived for the flooding velocity from flooding point experimental correlations reported in the literature. As far as open literature is concern, this attempt is first of its kind. In addition, this approach has been validated in this study by scaling between two existing pilot plants sizes, a similar demonstration could not be found in literature for reported scale-up studies of the process. The method developed in this study is used to scale up the pilot plant model developed in Aspen Plus® to a commercial CO_2 capture plant. And the results compared to scale-up study results obtained with the GPDC method.

2. Methodology

2.1 Model development

The closed-loop model of the CO_2 absorption and stripping process was developed in Aspen Plus® V8.4. The absorber and stripper model were developed using the RadFrac rate-based model The rate-based calculations give more reliable results in comparison to the equilibrium-based model counterpart (Lawal et al., 2009). This is because, in the rate-based model, equilibrium is assumed to be achieved only at the vapour-liquid interface and separation is caused by the mass transfer of component between the contacting phases. On the other hand, the equilibrium-based model assumed that each theoretical stage is made up of a well-mixed vapour and liquid phases in equilibrium with each other. This assumption is an approximation because, in real column, the contacting phases are never in equilibrium (Zhang et al., 2009).

The dimensions of the RadFrac columns were specified to be the same as those of the pilot plants as shown in Tables 4 and 6.

2.1.1 Thermodynamic and kinetic models

The liquid phase of the MEA-H_2O-CO_2 system is an electrolyte solution whose accurate modelling requires the selection of a base method that can account for the electrolytes in Aspen Plus®. The Electrolyte Non-Random-Two-Liquid (eNRTL) activity coefficient model (Chen and Evans, 1986) was used to calculate the activity coefficient and the SRK equation of state (Soave, 1972) was used to calculate the fugacity coefficient. Other important thermodynamic properties such as Henry's constant, vapour pressure, the heat of absorption and specific heat capacity are calculated using correlations within the eNRTL thermodynamic method in Aspen properties®. The equations describing the equilibrium reactions are defined as follows (Aspen Technology, 2008):

$$2H_2O \leftrightarrow H_3O^+ + OH^- \quad \text{(R1)}$$

$$CO_2 + 2H_2O \leftrightarrow H_3O^+ + HCO_3^- \quad \text{(R2)}$$

$$HCO_3^- + H_2O \leftrightarrow H_3O^+ + CO_3^{2-} \quad \text{(R3)}$$

$$MEACOO^- + H_2O \leftrightarrow MEA + HCO_3^- \quad \text{(R4)}$$

$$MEAH^+ + H_2O \leftrightarrow MEA + H_3O^+ \quad \text{(R5)}$$

The equilibrium constants for reactions R1 to R5 are calculated from the Gibbs free energy change, and the equilibrium reactions are assumed to occur in the liquid film. In the rate-based model, the reactions R6 and R7 representing the forward and backward reactions for the formation of bicarbonate and the reactions R8 and R9 representing the forward and backward reactions for the formation of carbamate are considered as kinetics-controlled reactions (Zhang and Chen, 2013).

$$CO_2 + OH^- \rightarrow HCO_3^- \quad \text{(R6)}$$

$$HCO_3^- \rightarrow CO_2 + OH^- \quad \text{(R7)}$$

$$MEA + CO_2 + H_2O \rightarrow MEACOO^- + H_3O^+ \quad \text{(R8)}$$

$$MEACOO^- + H_3O^+ \rightarrow CO_2 + H_2O + MEA \quad \text{(R9)}$$

The reaction rates for reactions R6 to R9 can be calculated by the power law which is described in Aspen Plus® by the following equation.

$$R_j = k_j^o T^n \exp\left[-\frac{E_j}{R}\left(\frac{1}{T}-\frac{1}{298.15}\right)\right]\prod_{i=1}^{N} C_i^{\alpha_{ij}} \qquad (1)$$

The values of k_j^o and E_j in equation 1 used for reactions R6 to R9 are shown in Table 1.

Table 1
Parameter of the pre-exponential factor and activation energy (Aspen Technology, 2008).

Reactions	Reaction direction	k^o_j (kmol/m^3 s)	E_j (kJ/mol)
R6	Forward	4.32 x 10^{13}	55.43
R7	Reverse	2.38 x 10^{17}	123.22
R8	Forward	9.77 x 10^{10}	41.24
R9	Reverse	2.18 x 10^{19}	59.19

2.1.2 Transport property models

Transport property models, namely density, viscosity, thermal conductivity, surface tension, and diffusivity have been calculated using the correlations summarised in Table 2.

Table 2
Summary of models for calculating transport properties (Aspen Technology, 2001).

Property	Gas-phase	Liquid phase
Density	COSTALD model by Hankinson and Thomson	Clark density model
Viscosity	Chapman-Enskog-Brokaw model	Jones-Dole model
Thermal conductivity	Wassiljewa-Mason-Sexena model	Riedel model
Surface tension		Onsager-samaras model
Diffusivity	Chapman-Enskog-Wilke-Lee model	Wilke-Chang model

2.1.3 Heat and mass transfer calculations

Heat and mass transfer calculations have been performed using correlations for the mass transfer coefficient, heat transfer coefficient, interfacial area, and the liquid holdup. A summary of the correlations is given in Table 3.

Table 3

Summary of correlations used for mass and heat transfers.

Correlations	References	
	Absorber	Stripper
Liquid and gas film mass transfer coefficient	Onda et al. (1968)	Bravo et al. (1985)
Heat transfer coefficient	Chilton and Colburn (1934)	Chilton and Colburn (1934)
Liquid holdup	Stichlmair et al. (1989)	Bravo et al. (1992)
Effective Interfacial area	Onda et al. (1968)	Bravo et al. (1985)

3. Model validation

In this study, pilot plant data from the Separation Research Programme (SRP) at the University of Texas at Austin, USA (Dugas, 2006) and the Brindisi CO_2 capture plant located in Brindisi, Italy (Enaasen, 2015) were used to validate the performance of the rate-based model presented in the previous section.

3.1 Model validation using the SRP pilot plant data

Experimental data collected at the SRP pilot plant which is a multifunctional test facility were used to validate the rate-based model. The SRP pilot plant uses synthetic flue gas produced by mixing air and CO_2 gas. The absorber and the stripper both have internal diameter of 0.427m and a total height of 11.1 m. The columns are each made up of two 3.05 m bed of packing with plate collector and liquid redistributor between them. It is capable of handling flue gas flow rate ranging from 330-830 m^3/h and can capture between 125 and 250 kg of CO_2/h. The main process conditions, dimensions of the absorbers and the strippers, and the type of packings used in the pilot plant for the three selected cases are summarized in Tables 4.

Table 4

Pilot plant data from the SRP CO_2 capture plant (Dugas, 2006)

Cases	28	32	47
Flue gas flow rate (m^3/min)	11.00	5.48	8.22
Flue gas CO_2 concentration (mol%)	16.54	17.66	18.41
Flue gas temperature (^oC)	47.98	46.56	59.23
Flue gas pressure (bar)	1.05	1.05	1.03
Lean solvent flow rate (m^3/min)	0.08	0.04	0.03
Lean solvent temperature (^oC)	40.00	40.56	40.07

Absorber pressure (bar)	1.00	1.00	1.00
Regenerator pressure (bar)	1.62	1.62	0.68
	Absorber	Stripper	
Diameter (m)	0.43	0.43	
Packing height (m)	6.10	6.10	
Packing type	IMTP 40	Flexipac 1Y	

The three experimental cases selected for model validation from the 48 experimental runs conducted at the SRP facility have different CO_2 concentrations and L/G ratios. Model validation was performed by comparing the model predictions for the CO_2 capture level and CO_2 loadings against experimental data for different feed conditions. The percentage CO_2 capture level and the CO_2 loading in the MEA solvent are calculated using Eqs. 2 and 3.

$$\text{Capture level (\%)} = \left(\frac{y_{CO_{2,in}} - y_{CO_{2,out}}}{y_{CO_{2,in}}}\right) * 100 \quad (2)$$

$$\text{Loading} = \frac{[CO_2] + [HCO_3^-] + [CO_3^{2-}] + [MEACOO^-]}{[MEA] + [MEA^+] + [MEACOO^-]} \quad (3)$$

Table 5 shows the model performance results against the experiment. There is a good agreement between the model predictions and the experiment data for all the variables outlined in Table 5. The percentage relative errors (PRE) of the model prediction against the experimental data are calculated as follows:

$$\text{PRE} = \frac{\left|i_{\text{experiment}} - i_{\text{model}}\right|}{i_{\text{experiment}}} * 100 \quad (4)$$

Fig.1 presents the comparison between the measured and predicted liquid phase temperature profiles along the height of the absorber and the stripper. The model generally gives a good prediction of the temperature profiles in the absorber and the stripper for the three selected cases. Also, the model accurately predicted the location of the temperature bulge (maximum temperature) in the absorber for the three cases as illustrated by curves a, c and e). The location and magnitude of the temperature bulge depend on L/G ratio (Plaza and Rochelle, 2011). Dugas (2006) found that the temperature bulge was located at the top of the absorber with L/G

less than 5 kg/kg and at the bottom with L/G greater than 6 kg/kg. This explains the location of the temperature bulge close to the bottom of the absorber packing for curves a and c (L/G=6.6 kg/kg) and close to the top of the absorber packing for curve e (L/G=3.4 kg/kg).

Table 5

Model performance against experimental data for the SRP CO_2 capture pilot plant

Cases	Lean loading (mol CO_2/mol MEA)			Rich loading (mol CO_2/mol MEA)			CO_2 capture level (%)		
	Exp.	Model	PRE (%)	Exp.	Model	PRE (%)	Exp.	Model	PRE (%)
28	0.28	0.28	0.00	0.41	0.41	0.00	86	85	1.16
32	0.27	0.27	0.00	0.43	0.43	0.00	95	90	5.26
47	0.28	0.30	-6.60	0.53	0.48	9.43	69	69	0.00

(a)

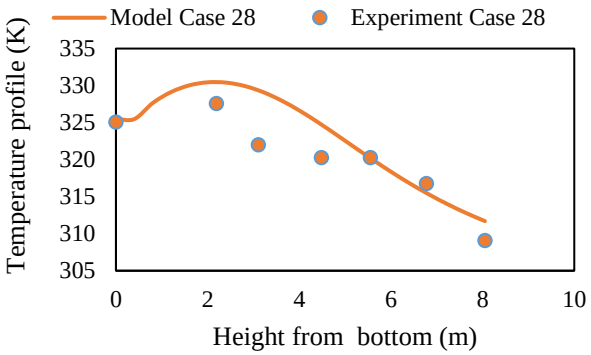

(b)

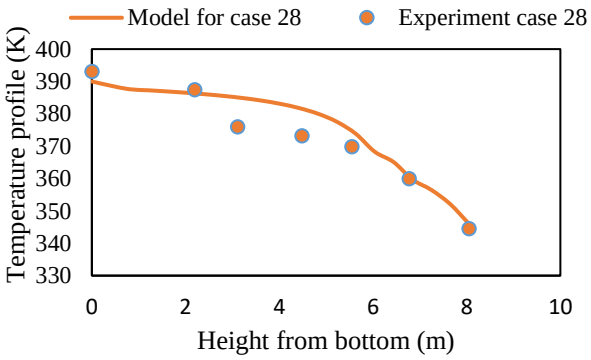

(c)

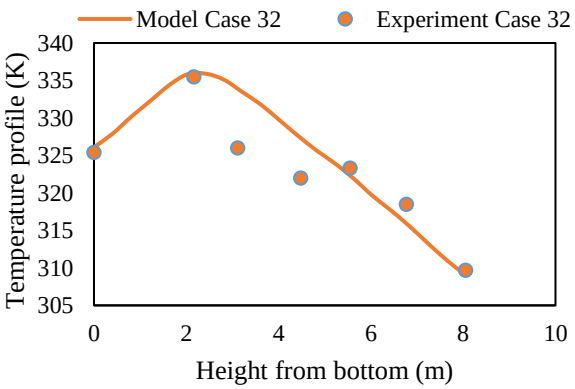

(d)

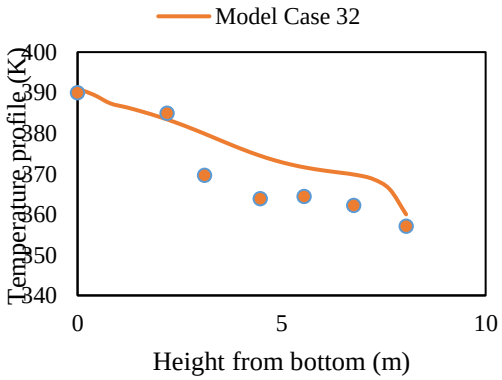

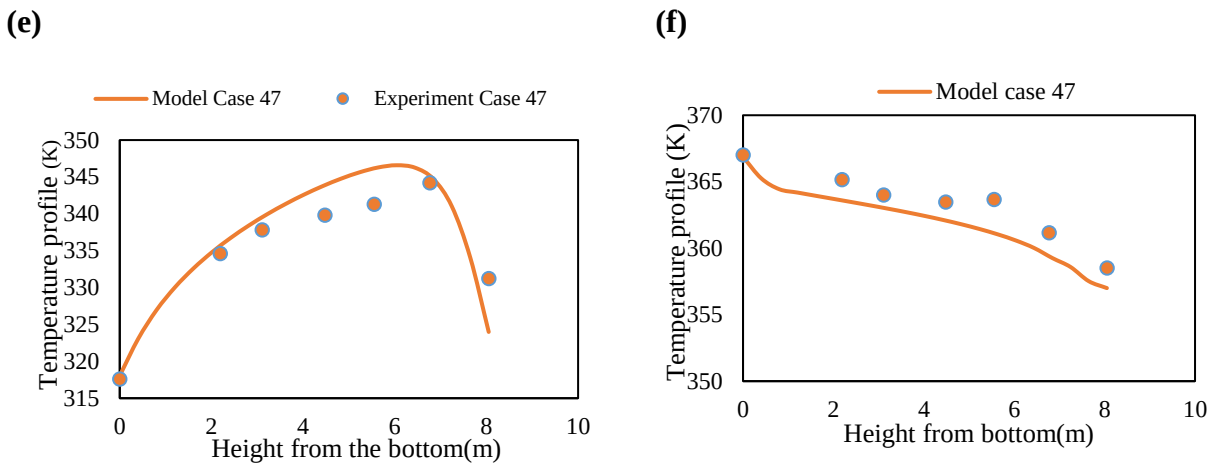

279 **Fig. 1.** Model predictions against experimental data for temperature profiles in the absorber (a,
280 c, e) and in the stripper (b, d, and f) of the SRP pilot plant for the three cases.
281
282 **3.2 Model validation using the Brindisi pilot plant data**
283 The rate-based capture model was also validated using experimental data collected at the
284 Brindisi pilot plant (Enaasen, 2015). It is a relatively large plant compared to the SRP pilot
285 plant described in section 3.1. The pilot plant uses a flue gas produced from one of the four
286 units (each with capacity of 660 MW_e) of a coal-fired power plant. The absorber and stripper
287 have diameters of 1.5m and 1.3m, and packing heights of 22m and 11m respectively. It can
288 capture up to 2500 kg of CO_2/h from a flue gas slipstream and has a maximum capacity of 9212
289 m^3/h which corresponds to about 0.45 % of the total flue gas produced from the unit four of
290 the power plant (Lemaire et al., 2014). The solvent flow rate can be varied between 20-80 m^3/h.
291 The main process conditions, dimensions of the absorbers and the strippers, and the type of
292 packings used in the pilot plants for the selected cases are summarized in 6.

293 **Table 6**
294 Pilot plant data from the Brindisi CO_2 capture plant (Enaasen, 2015).

Cases	2	3	4	5	7
Flue gas flow rate (Nm^3/h)	9876	9929	9893	9949	9921
Flue gas CO_2 concentration (dry vol%)	11.00	12.50	12.00	10.40	11.00
Flue gas temperature (^oC)	46.20	44.80	45.60	44.70	46.90
Lean solvent flow rate (m^3/h)	30	30	30	35	35
Lean solvent temperature (^oC)	46.90	47.00	47.00	47.00	47.10
Lean solvent MEA concentration (wt%)	29.60	29.80	29.80	29.80	29.70
	Absorber		Stripper		

Diameter (m)	1.50	1.30
Packing height (m)	22	11
Pressure (bar)	1.00	1.84

Five experimental cases (Table 6) with the least relative deviations in steady-state CO_2 mass balance were selected for the model validation among the 12 experimental cases reported. Two sets of packings were used in the absorber and stripper during the model validation. The first set of packing (Mellapak 250X and IMTP 50) is the original packings used in the Brindisi pilot plant during the experiments while the second set of packing (IMTP 40 and Flexipac 1Y) is the packing used in the SRP pilot plant. This was done to:

1. Enable the scale-up from the SRP pilot plant to the Brindisi pilot plant in order to validate the proposed scale-up approach presented later in section 4.
2. Enable the scale-up of the Brindisi pilot plant model (using the second set of packing) to a commercial CO_2 capture plant (Section 5.2) using the proposed scale-up method. The results obtained from the scale-up will be compared to those obtained from a commercial CO_2 capture plant designed by Canepa et al. (2013) using the same set of packings and the GPDC method.

The parity plot of the rich solvent CO_2 loading, desorbed CO_2 and specific duty predicted by the model using the two sets of packings against experimental data are shown in Figs. 2-4. The validation results show good agreement between the model predictions and experimental data. The results further demonstrate that the sets of packing used in the columns have identical performance in terms of rich CO_2 loading, amount of CO_2 desorbed and specific duty.

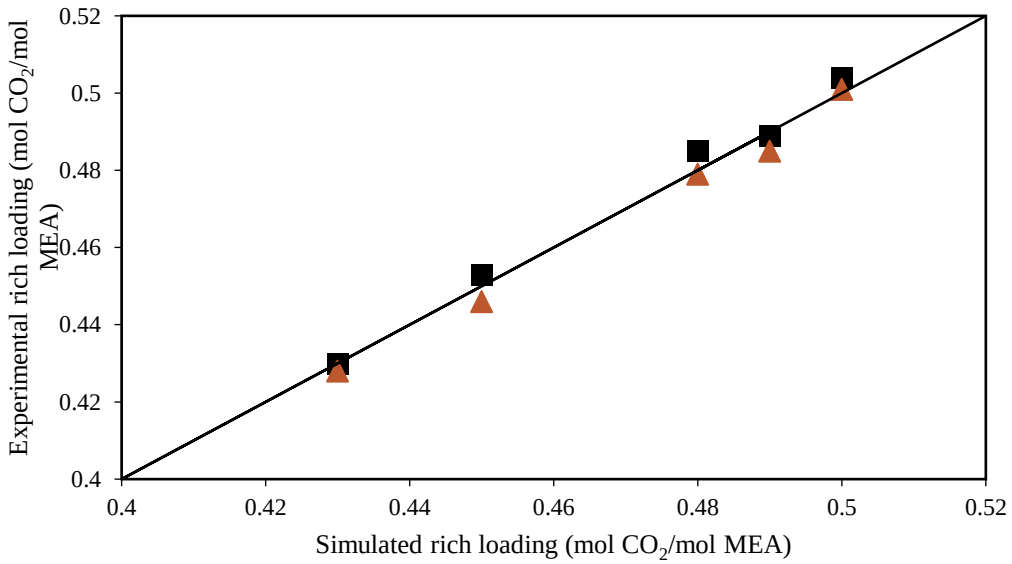

Fig. 2. Experimental values of rich loading (Enaasen, 2015) compared to simulated values obtained with set 1 packing (■) and set 2 packing (▲) and the dark line represents equal experimental and simulated rich loadings.

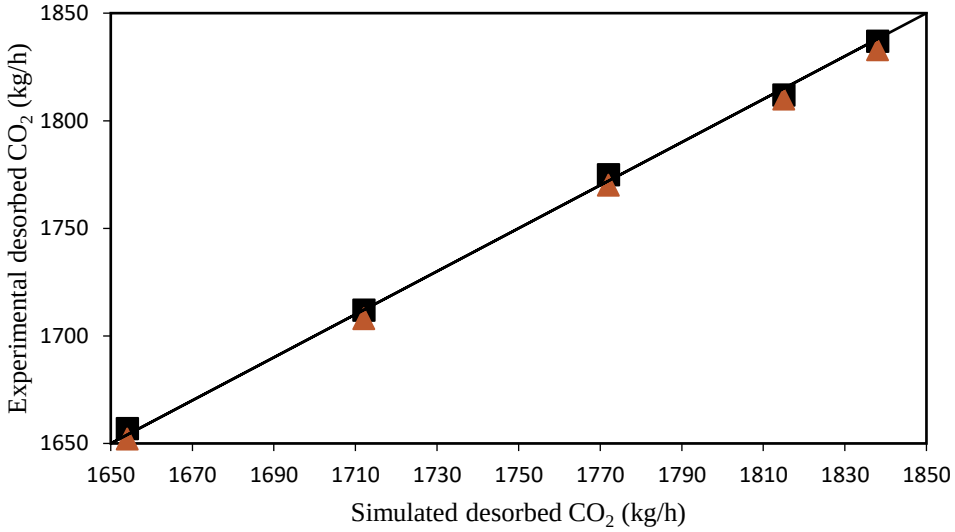

Fig. 3. Experimental values of desorbed CO_2 (Enaasen, 2015) compared to simulated values obtained with set 1 packing (■) and set 2 packing (▲). The dark line represents equal experimental and simulated desorbed CO_2.

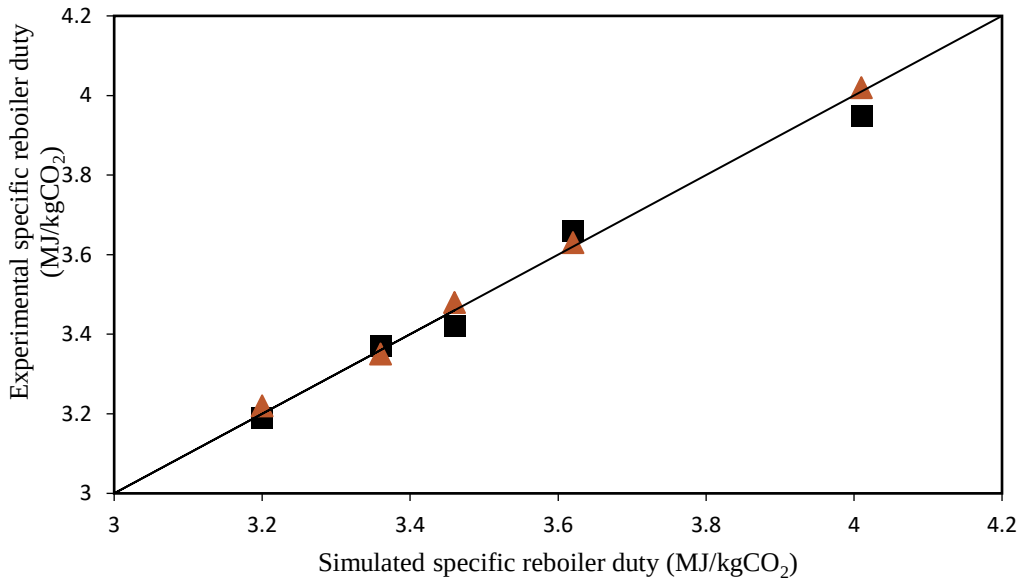

Fig. 4. Experimental values of specific duty (Enaasen, 2015) compared to simulated values obtained with set 1 packing (■) and set 2 packing (▲), the dark line represents equal experimental and simulated specific duty.

4. A newly proposed method for estimating the diameter of absorber and stripper

The diameter of a packed column is a key parameter that must be determined in the design of a packed bed absorber or stripper. The columns are designed in such a way to avoid flooding because flooding reduces their efficiency and sometimes causes the column to breakdown (Liu et al., 2019). Since the flooding point establishes the upper limit of the hydrodynamic capacity at which the packed column can operate, the velocity of the gas at flooding condition is particularly important and is a vital design parameter for the packed column (Brunazzi et al., 2008). Sherwood et al. (1938) developed the first generalized correlation chart for predicting flooding points in random dumped packings using experimental data from an air-water system. The chart which contained only one curve was later modified by Lobo et al. (1945). The ordinate of the chart includes the ratio a/ε^3 for characterising the packing size and shape. Leva (1954) added several isobaric curves to determine the pressure drop in the packed beds. In addition, Leva (1954) determined that the ratio a/ε^3 did not adequately predict the packing hydraulic performance and proposed the use of packing factor to characterise packing size and shape. Eckert (1970) further modified the chart and calculated the packing factor from experimentally determined pressure drops. The modified Eckert version (Fig. 5), known as the Sherwood-Leva-Eckert (SLE) GPDC chart has been the standard for pressure drop and flooding points prediction in a column packed with random packings for many decades.

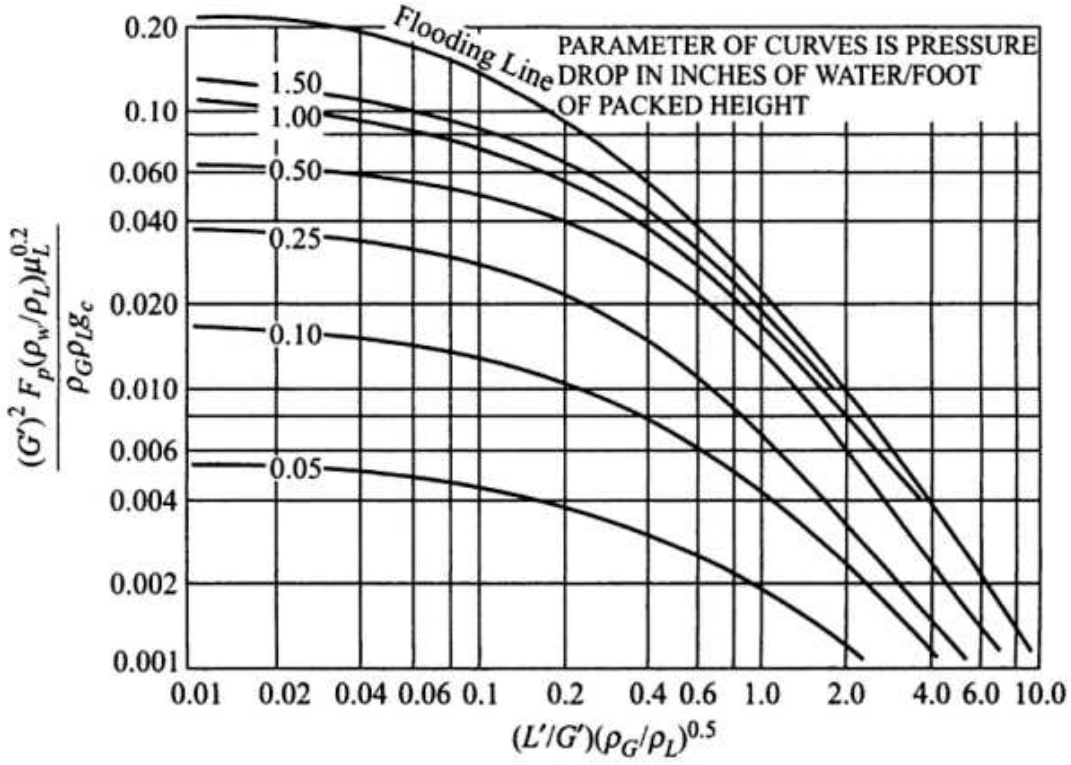

Fig. 5. Generalized pressure drop correlation for packings (Eckert, 1970)

In later versions of the GPDC chart developed by Strigle (1994) for random packings and Kister et al. (2007) for structured packings, only the pressure drop curves were retained while the flooding curve was omitted (Wolf-Zöllner et al., 2019a). Kister and Gill (1991) developed a correlation for predicting the flooding point and pressure drop in packed columns and an expression for the flooding curve was written in equation form particularly for the relationship between the abscissa and the ordinate as follows (Piché et al., 2001).

$$CP = A\log^2(F_{LV}) + B\log(F_{LV}) + C \tag{5}$$

Where F_{LV} is the flow parameter. It is the ratio of the kinetic energy of the liquid to the kinetic energy of the gas entering the packed column (Kister et al., 2007), and it is represented as follows:

$$F_{LV} = \frac{L}{G}\sqrt{\frac{\rho_L}{\rho_G}} \tag{6}$$

The value of the flow parameter is low for vacuum operation but high for operations involving high pressures or high liquid/vapour loading such as gas absorption operation. The CP in Eq. 5 is the capacity parameter and it is given by:

$$CP = \sqrt{V_{G,fl}^2\left(\frac{\rho_G}{\rho_L - \rho_G}\right)v^{0.1}F_P} \tag{7}$$

The pressure drop at which incipient flooding occurs in columns packed with modern random packings has been correlated and expressed as a function of the packing factor F_p by Kister and Gill (1991) as shown by Eq. 8.

$$\Delta P_{fl} = 0.115F_P^{0.7} \tag{8}$$

Eq.8 also applies to structured packings and has been found to predict very well the pressure drop at flooding point for structured packings (Geankoplis, 2014; Kister and Gill, 1992). The equation is particularly applicable to packings with F_P between 10 and 60 ft^{-1}, thus, it is capable of predicting the pressure drop at flooding in packed columns from as low as 0.57 in. H_2O/ft

for packings with F_p of 10 ft^{-1} to as high as approximately 2 in. H_2O/ft for packings with F_P of 60 ft^{-1}. However, the equation only gives an optimistic prediction of the flooding point pressure drop at F_p beyond 60 ft^{-1} and should therefore not be used with F_P above this value (Geankoplis, 2014).

The expressions for determining the parameters A, B and C in Eq.5 together with their range of application are summarised in Table 7. These parameters are determined using the flooding point pressure drop calculated from Eq. 8.

Table 7

Expressions for parameters in Eq.5 (Piché et al., 2001)

Parameters	Expression	Range of application
A	$0.07\ln(\Delta P_{fl}) - 0.11$	$0.5 \leq \Delta P_{fl} \leq 5.0$ inH_2O/ft
B	$-0.25\ln(\Delta P_{fl}) - 0.89$	$0.5 \leq \Delta P_{fl} \leq 1.0$ inH_2O/ft
B	-0.89	$1.0 \leq \Delta P_{fl} \leq 5.0$ inH_2O/ft
C	$0.12\ln(\Delta P_{fl}) + 0.71$	$0.5 \leq \Delta P_{fl} \leq 5.0$ inH_2O/ft

Eq. 5 can be re-written in the form shown below;

$$CP = A(\log F_{LV})^2 + B\log(F_{LV}) + C \qquad (9)$$

By equating Eqs. 7 and 9 and substituting for F_{LV} in the resulting equation. An expression of the form in Eq 10 can be written for the flooding velocity ($V_{G,fl}$).

$$V_{G,fl} = 0.3048\left[\left(\frac{\rho_G}{\rho_L - \rho_G}\right)^{-0.5} \nu^{-0.05}\, F_P^{-0.5}\left\{A\left(\log\left(\frac{L}{G}\sqrt{\frac{\rho_G}{\rho_L}}\right)\right)^2 + B\left(\log\left(\frac{L}{G}\sqrt{\frac{\rho_G}{\rho_L}}\right)\right) + C\right\}\right] \qquad (10)$$

The flooding velocity (upper limit of the rate of gas flow) in a packed column can be calculated from Eq.10 once process information such as the flow rate, density and kinematic viscosity of the individual phase are known. Also important is the packing factor. The values of the density and kinematic viscosity can be obtained from open literature, experiments or chemical process simulation software such as Aspen Plus® and ProMax. Eq. 10 has limitation over the range of its application. This is because the correlation presented in Eq. 8 which formed the basis of the equation only gives a good prediction of the flooding point pressure drop between F_P range of

10 to 60 ft^{-1}. Therefore, it is recommended that it should only be used to estimate the flooding velocity in a column packed with packings with F_P in the range specified above.

The diameter required by a given gas and liquid flow rate in a packed column is based on the maximum allowable pressure drop and the maximum operational capacity (MOC). The values for the MOC can range from 60 to 86 percent, thus, packed columns are usually designed to operate at about 60-80 percent of the flooding velocity(Marx-Schubach and Schmitz, 2019). In this work, it is assumed that the column operates at 70 percent of the flooding velocity, hence the superficial gas velocity at operating condition was calculated as follows:

$$V_G = 0.7V_{G.fl} \tag{11}$$

The diameter of the column required to perform the absorption operation at 70% of flooding velocity can be calculated from the expression in Eq. 12.

$$D = \sqrt{\frac{4G}{\pi V_G \rho_G}} \tag{12}$$

5. Model Scale-up

The design of a commercial PCC plant by the scale-up of PCC pilot plant model requires scale-up calculations to be performed to determine the size of the absorber and the stripper. One important parameter that determines the size of these columns is the amount of flue gas to be treated by the commercial PCC plant. In most cases, the flue gas is thousands of times the amount at pilot scale. For instance, the commercial PCC plant designed by Lawal et al. (2012) and Canepa et al. (2013) process about 5000 and 2200 times the amount of flue gas at the pilot scale. Considering that the CO_2 capture process generally involves many interacting variables, accurate scale-up of the process to a commercial PCC plant that is capable of processing flue gas that is thousands of times the amount at pilot scale is, therefore, a very complicated exercise. To avoid this complication, a two-stage scale-up of the validated models presented in section 3 is carried out as follows:

(1) The validated model of the SRP CO_2 capture pilot plant (flue gas flow rate 0.15 kg/s) is scaled up to the size of the Brindisi CO_2 capture pilot plant (flue gas flow rate 3.22 kg/s) to validate the proposed scale-up method.

(2) The validated model of the Brindisi pilot plant is scaled up to a commercial CO_2 capture plant capable of serving a 250 MW_e CCGT power plant producing 356 kg/s of flue gas.

5.1 Scale-up of the SRP CO_2 capture pilot plant to the Brindisi CO_2 capture pilot plant

In order to validate the approach proposed in section 4, the SRP pilot plant is scaled up to the size of the Brindisi pilot plant. Based on the amount of flue gas processed, the Brindisi pilot plant has the capacity that is about 22 times of the SRP pilot plant. It is a relatively large PCC pilot plant that is attached to a full-scale coal-fired power plant and operated on flue gas from the power plant. The steps involved in the scale-up calculations are provided in the following subsections:

5.1.1 Estimation of lean solvent flow rate

The lean solvent flow rate required to capture 90% of the CO_2 in the flue gas entering the absorber of the Brindisi pilot plant is estimated based on the absorption capacity of 0.2 mol CO_2/mol MEA, lean solvent MEA concentration of 30 wt%, CO_2 mass fraction of 0.1608 and flue gas mass flow rate of 3.22 kg/s. The estimation is carried out by assuming a constant flow rate for the gas and the solvent throughout the absorber column. The lean solvent flow rate required for the absorption operation is estimated using the approach of Agbonghae et al. (2014) presented in Eq. 13.

$$L_{Lean} = \frac{G x_{CO_2} \varphi_{CO_2}}{100 z(\alpha_{Rich} - \alpha_{Lean})} \left[\frac{M_{MEA}}{44.009}\left(1 + \frac{1 - \omega_{MEA}}{\omega_{MEA}}\right) + z\alpha_{Lean}\right] \quad (13)$$

With regard to the stripper, the total solvent flow is equivalent to the sum of the mass flow rate of the rich solvent and reflux rate while the gas flow rate is equivalent to the boil-up rate needed to maintain the CO_2 loading in the lean solvent at 0.23 CO_2/per mole MEA. Based on these calculations, the solvent flow rate to the absorber and stripper was estimated to be 10.88 kg/s and 11.5 kg/s respectively. The gas (vapour) phase required for the desorption of CO_2 was estimated to be 1.62 kg/s.

5.1.2 Estimation of columns diameter

The diameter of the absorber and the stripper is estimated using Eqs. 10 to 12 presented in section 4. Information regarding the density and kinematic viscosity of the MEA solvent was obtained from the SRP pilot plant model. Column packings used in the SRP pilot plant were adopted in the Brindisi plant. The absorber was packed with IMTP 40 with F_P of 78.7 m^{-1} (24 ft^{-1}) and the stripper was packed with Flexipac 1Y with F_P of 168.3 m^{-1} (51.3 ft^{-1}). Using the given flue gas and the estimated solvent flow rates together with the values of parameters provided in Table 8, the superficial gas velocities in the absorber and the stripper were estimated from the flooding gas velocity as 1.83 and 1.20 m/s respectively.

Table 8

Parameters used to estimate the flooding velocity in the absorber and the stripper

Parameter	Absorber	Stripper
ρ_L (kg/m^3)	1017.06	1019.88
ρ_G (kg/m^3)	1.03	1.02
A	-0.11	-0.07
B	-0.91	-0.89
C	0.72	0.79

Based on the gas velocities, the diameter of the absorber and the stripper were calculated from Eq. 12 to be 1.46 m and 1.28 m respectively. The values obtained for the absorber and the stripper diameter are similar to the values of 1.5 m and 1.3 m reported for the absorber and the stripper of the Brindisi pilot plant. The percentage deviations of the estimated column diameters from those of the Brindisi pilot plant are 2.6 % and 1.54 %, which are within an acceptable range. The fact that the method proposed herein is able to estimate the diameter of the absorber and the stripper of an existing plant validates the approach and demonstrates that it can confidently be used to estimate the diameter of a column required for an absorption process.

5.1.3 Estimation of packing height

The height of packing (Z_T) require for a given separation in a packed column is most often expressed in terms of the overall gas-phase mass transfer coefficient and the gas composition. Based on this, the packing height of the column can be calculated with the expression (Seader et al., 2006).

$$Z_T = \frac{G_i}{K_G aP} \int_{yco_{2,in}}^{yco_{2,out}} \frac{dy}{y - y^*} \quad (14)$$

The right-hand side of Eq.14 can be written more conveniently as a product of two terms involving the height and number of transfer units.

$$Z_T = H_{OG}.N_{OG} \quad (15)$$

The N_{OG} is the number of (gas) transfer units and can be expressed as:

$$N_{OG} = \int_{yco_{2,in}}^{yco_{2,out}} \frac{dy}{y - y^*} = In\left(\frac{y_{CO_{2,in}}}{y_{CO_{2,out}}}\right) \quad (16)$$

The larger the value of N_{OG}, the higher the height of the packed column needed to achieve the required separation. Eq. 16 assumes that the term y^* which is the concentration of CO_2 in equilibrium with the bulk concentration is negligible because of the fast reaction between CO_2 and the MEA solution and because of the negligible equilibrium partial pressure of CO_2 (Aroonwilas and Veawab, 2004; Fu et al., 2014; Khan et al., 2011).

The H_{OG} is the height of a transfer unit, it shows the efficiency of the packing i.e. the smaller the value of H_{OG} the more efficient the contacting (Coulson and Richardson, 2002). The value of H_{OG} was computed by:

$$H_{OG} = \frac{G_i}{K_G aP} \quad (17)$$

Dugas (2006) in a series of experiments performed at the SRP pilot plant reported the mass transfer performance of the packing (IMTP 40) in terms of K_Ga in the absorber used to absorb CO_2 from the flue gas using MEA. The concentrations of the MEA in the solvent and CO_2 in the flue gas, as well as the operating conditions i.e. temperature and pressure used to obtain the K_Ga values are similar to that of the Brindisi pilot plant. Considering that the same packing is used in the Brindisi pilot plant, the K_Ga values are not expected to change markedly. In view of this, the K_Ga values reported by Dugas (2006) were used to estimate the H_{OG} of the absorber.

Based on the above, the packing height (Z_T) of the absorber was estimated to be 22.55 m using the values of the parameters summarised in Table 9.

Table 9

Calculated values of parameters used to estimate the absorber packed bed

Parameters	Value
N_{OG}	4.1
K_Ga (kmol/m^3 s. bar)	1.22 x 10^{-2}
G_i (kmol/s m^2)	0.06
P (bar)	1.00
H_{OG} (m)	5.50

The packing height of the stripper could not be determined using the same approach for the absorber because the K_Ga values for the runs with the Flexipac 1Y in the stripper were not reported (Dugas, 2006). During the experiments, negative CO_2 driving force was encountered at the top of the stripper, that made it impossible to calculate the log mean driving force and the mass transfer coefficient of the Flexipac 1Y packing. Therefore, the packing height of the stripper was determined using a different approach that involves the summation of the HETPs of stages in the stripper. This is the same approach used in Agbonghae et al. (2014) to estimate the stripper packing height. The packing height of a stripper with N number of stages can be estimated as follows; (Agbonghae et al., 2014).

$$Z_{T,Stripper} = \sum_{i=2}^{N-1} HETP_i \qquad (18)$$

The approach was implemented using the calculator block in Aspen Plus® to automatically adjust the ending stage number of the packed section to the number of stages while fixing the starting stage of the packed section. The starting stage for the stripper was fixed at 2, also a design specification for the lean loading was set at 0.23 mol CO_2/mol MEA. Starting with a generic total stage number of 5, the number of stages in the stripper was continuously increased by 1, till a certain point where a further increase had a negligible effect on the reboiler duty. Using this approach, the packing height of the stripper was determined to be 11.4 m. Details of this approach can be obtained is available in Agbonghae et al. (2014). Table 10 shows how the

scale-up result for the diameter and packing height of the absorber and stripper compare with the pilot plant.

Table 10

Comparison of results between the scale-up and the pilot plant measurement

	Pilot plant		Scale-up	
	Absorber	Stripper	Absorber	Stripper
Diameter (m)	1.50	1.30	1.46	1.28
Height (m)	22	11	22.55	11.40

5.2. Scale-up of the Brindisi CO_2 capture plant to commercial CO_2 capture plant

Having applied the approach to scale-up between existing capture plants in section 5.1, the Brindisi CO_2 capture plant was scaled up to deal with the flue gas equivalent to that discharge by a 250 MW_e CCGT power plant described in Canepa et al. (2013). Based on the amount of flue gas processed, the capacity of the commercial CO_2 capture plant is about 110 times that of the Brindisi CO_2 capture plant. The operating conditions of the columns and the input conditions of the flue gas after treatment to remove acid gases, oxygen and particulates matter are given in Table 11. These conditions were chosen to be the same as those reported for the case without exhaust gas recirculation in Canepa et al. (2013). This was done to enable the comparison of results obtained from this study with those obtained from that study Canepa et al. (2013) who had previously scaled up from the SRP pilot plant based on these same conditions using the GPDC method and assumed pressure drop of 412 Pa/m of packing.

Table 11

Inlet conditions of the PCC capture plant (Canepa et al., 2013)

Compositions (Mass fraction)	Value
CO_2	0.076
H_2O	0.047
N_2	0.862
Argon	0.015
Flue gas temperature (K)	313
Lean solvent temperature	313
Lean MEA concentration (wt%)	30
CO_2 Capture level (%)	90
Mass flow rate (kg/s)	356
Absorber pressure (kPa)	101
Absorber packing type	IMTP no. 40

Stripper pressure (kPa)	162
Stripper packing type	Flexipac 1Y

Going by the CO_2 mass fraction, flue gas mass flow rate, lean MEA concentration and the CO_2 capture level in Table 11, the solvent flow rate required by the commercial CO_2 capture plant to treat the flue gas was estimated with Eq. 13. The amount of solvent flow required is dependent on its absorption capacity. The impact of the absorption capacity ($\Delta\alpha$) on the solvent flow rate required by the commercial CO_2 capture plant is shown in Fig. 6. The solvent flow rate to the absorber was estimated to be 669 kg/s. Likewise, the solvent flow rate to the stripper was obtained to be 583 kg/s while the vapour flow rate (boiled-up rate) was obtained to be 58 kg/s.

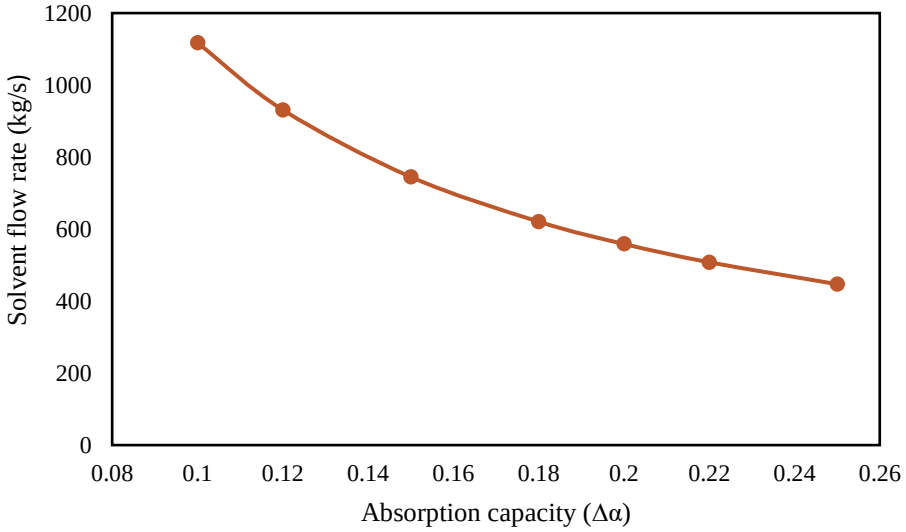

Fig. 6 Solvent flow rate at different absorption capacity

The diameter of the absorber and the stripper required by the commercial CO_2 capture plant were determined as earlier illustrated in section 5.1.2 using Eqs. 10 – 12. Physical properties such as density and kinematic viscosity useful for calculation were obtained from the Brindisi CO_2 capture pilot plant model simulation. The flooding velocity ($V_{G,fl}$) and the operating superficial gas velocity V_G were determined to be 3.25 m/s and 2.27 m/s in the absorber, and 1.83 m/s and 1.28 m/s in the stripper respectively. The vapour flow rate was far lower in the stripper than in the absorber thereby making the rich amine flow rate the deciding factor in the design, hence a smaller diameter than the absorber.

Based on the superficial gas velocities in the columns, the diameter of the absorber and the stripper required by the commercial CO_2 capture plant was determined to be 13.86m and 7.50 m respectively. The relationship between the diameter and the number of columns required by

the capture plant is presented in Fig. 7. This was based on what can be delivered by the state-of-the-art technology and maximum column diameter of 18 m for a commercial CO_2 capture plant (IEA-GHG, 2006; Reddy et al., 2013, 2008; Scherffius et al., 2013). Moreover, absorbers of similar diameter have been designed and built by Fluor just as strippers of similar diameter have been constructed and used for SO_2 stripping in power plants (Dutta et al., 2017; Reddy et al., 2008).

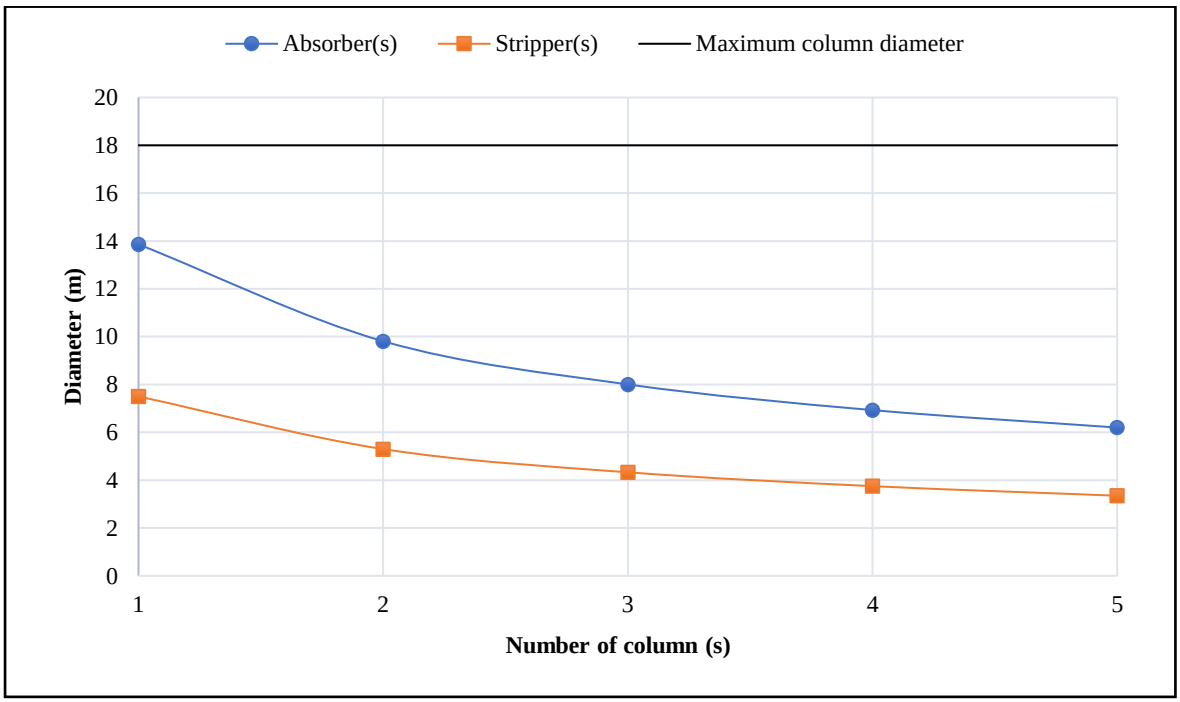

Fig. 7 Relationship of the diameter of columns and the number of columns

The diameter calculated for the absorber and the stripper in this study was found to be below this value. As a result, a single absorber and a single stripper were selected for the commercial-scale CO_2 capture plant in order to minimize the number of absorption trains and reduce the complexity of the plant. As a consequence, the plant footprint and capital cost are reduced. The packing height of 28.5 m was arrived at for the absorber using the approach presented in section 5.1.3. This same value of packing height was used for the stripper.

6. Simulation of the commercial CO_2 capture plant

The commercial-scale CO_2 capture plant was simulated in Aspen Plus® V8.4 and the flowsheet that was developed for the plant in this work is shown in Fig. 8. The comparison of results obtained from the final simulation with Canepa et al. (2013) is presented in Table 12.

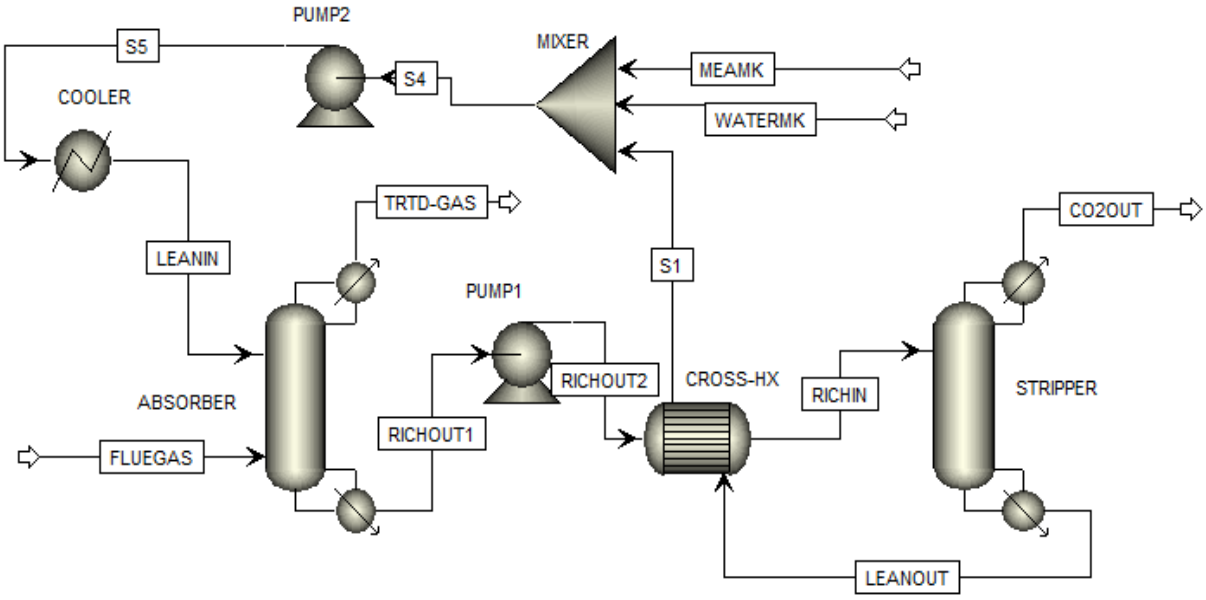

Fig. 8 Process flowsheet of the commercial CO_2 in Aspen Plus®

It can be observed from Table 12 that this study achieves lesser equipment size than those reported in Canepa et al. (2013) for the absorber and the stripper columns. In Canepa et al. (2013), two absorbers each of diameter 9.5 m and a stripper of diameter 8.2 m were required by the CO_2 capture plant to treat flue gas from a 250 CCGT power plant. In this study, a single absorber and stripper of diameters 13.86 m and 7.5 m respectively were designed for the same capture plant. The higher column diameter reported by Canepa et al. (2013) might be due to the pressure drop of 412 Pa/m packing assumed in columns sizing is higher than the actual pressure drop in the absorber and the stripper of a CO_2 capture plant for a 250 CCGT power plant.

Table 12

Comparison of key results obtained from this work with those obtained by Canepa et al. (2013)

	Canepa et al. (2013)	Results from this work
Lean solvent flow rate (kg/s)	720.46	705.23
L/G ratio (mol/mol)	2.29	2.23
Lean solvent loading (mol CO_2/mol MEA)	0.30	0.30
Rich solvent loading (mol CO_2/mol MEA)	0.45	0.47
CO_2 capture level (%)	90	90
Flooding ratio (%)	Not reported	70
Absorber		
Number of absorbers	2 [a]	1
Absorber packing	IMTP no. 40	IMTP no. 40
Absorber diameter (m)	9.50	13.86
Absorber packing height (m)	30	28.50
Absorber pressure drop (Pa/m)	412	241
Stripper		
Number of strippers	1	1
Stripper diameter (m)	8.20	7.50
Stripper packing height (m)	30	28.50
Stripper pressure drop (Pa/m)	412	57
Reboiler temperature (^oC)	117	115.70
Reboiler duty (MW)	121	115.30
Specific duty (GJ/tonCO_2)	4.97	4.69
Condenser temperature (^oC)	25	25

[a] A single absorber will result in diameter of 14.10 m.

The commercial-scale CO_2 capture developed in this study achieved a pressure drop of 241 Pa/m and 57 Pa/m of packing in the absorber and in the stripper respectively. The pressure drop in the stripper is much lower than the absorber because the vapour flow in the stripper is much lower and the structured packing used in the stripper is expected to provide lower gas-phase pressure drop than the random packing used in the absorber. The pressure drop in the absorber and the stripper are less for this study indicating a reduction in power loss due to pumping which would translate to a reduction in the operational costs of the capture process.

Meanwhile, the absorber and the stripper packing height in this study are also smaller. Canepa et al. (2013) reported the same packing height of 30 m for the absorber and the stripper in their study without giving the details of how the values were arrived at. This was despite using a structured packing (Flexipac 1Y) with higher mass transfer efficiency and lower HETP (which should reduce packing height) in the stripper. The results in this study will support more

accurate estimation of the capital cost of the process since according to Abu-Zahra et al. (2007) the absorber and the stripper account for about 55% and 17% of the total equipment purchase cost for the whole CO_2 capture process. The specific duty of the CO_2 capture plant attained a value of 4.69 GJ/ton CO_2 representing a 5.63% reduction in the value reported by Canepa et al. (2013). The solvent flow rate is also less for this study because more CO_2 is absorbed as reflected in the rich loading which is slightly higher in this study. The lower solvent flow rate would reduce the energy consumption for pumping and regeneration thereby reducing the operating cost of the process.

7. Conclusions

A steady-state model for the solvent-based post-combustion CO_2 capture plant using MEA has been developed and validated at pilot scale in Aspen Plus®. The validation results showed good agreement between the model predictions and the pilot plants measurements. A new scale-up method for estimating packed column diameter based on the use of flooding gas velocity is proposed in this paper. The scale-up method was validated by applying it to the scale-up between two existing pilot plant sizes. The method was able to estimate the diameter of the absorber and the stripper with deviations of 2.6 % and 2.54 % respectively. The validation showed that the method could be used to estimate the diameter of the packed column used in the CO_2 capture process. Furthermore, it was used to scale up the validated model from pilot scale to commercial scale to process flue gas from a 250 MW_e CCGT power plant. The results obtained show that estimates using the GPDC method in literature may be significantly higher than required. In addition, with our approach, it was found that for commercial-scale cases, the solvent flow rate and energy consumption were less by about 2.12% and 5.63% compared to the GPDC approach. Therefore, the capital and operating costs for the process using the newly proposed scale-up method could be lower based on our estimates of the column dimensions, solvent flow rate and specific reboiler duty.

Acknowledgment

The authors would like to gratefully acknowledge the financial support of the project from the Petroleum Technology Development Fund (PTDF), Nigeria.

References

Abu-Zahra, M.R.M., Niederer, J.P.M., Feron, P.H.M., Versteeg, G.F., 2007. CO_2 capture from

power plants. Part II. A parametric study of the economical performance based on mono-ethanolamine. Int. J. Greenh. Gas Control 1, 135–142.

Agbonghae, E.O., Hughes, K.J., Ingham, D.B., Ma, L., Pourkashanian, M., 2014. Optimal process design of commercial-scale amine-based CO2capture plants. Ind. Eng. Chem. Res. 53, 14815–14829.

Aroonwilas, A., Tontiwachwuthikul, P., Chakma, A., 2001. Effects of operating and design parameters on CO_2 absorption in columns with structured packings. Sep. Purif. Technol. 24, 403–411.

Aroonwilas, A., Veawab, A., 2004. Characterization and Comparison of the CO_2 Absorption Performance into Single and Blended Alkanolamines in a Packed Column. Ind. Eng. Chem. Res. 43, 2228–2237.

Aspen Technology, 2008. Rate-based model of the CO_2 capture process by MEA using Aspen plus. Burlington, MA.

Aspen Technology, 2001. Physical property methods and models 11.1. Cambridge, MA.

Awoyomi, A., Kumar, P., Edward, A., 2019. CO_2/SO_2 emission reduction in CO_2 shipping infrastructure. Int. J. Greenh. Gas Control 88, 57–70.

Biliyok, C., Yeung, H., 2013. Evaluation of natural gas combined cycle power plant for post-combustion CO_2 capture integration. Int. J. Greenh. Gas Control 19, 396–405.

Bravo, J, L. Rocha, J, A. Fair, J, R., 1985. Mass transfer in Gauze Packings. Hydrocarb. Process 64, 91–95.

Bravo, J.L., Patwardhan, A.A., Edgar, T.F., 1992. Influence of Effective Interfacial Areas in the Operation and Control of Packed Distillation Columns. Ind. Eng. Chem. Res. 31, 604–608.

Brunazzi, E., Macías-Salinas, R., Viva, A., 2008. Calculation Procedure for Flooding in Packed Columns Using a Channel Model. Chem. Eng. Commun. 196, 330–341.

Bui, M., Gunawan, I., Verheyen, V., Feron, P., Meuleman, E., Adeloju, S., 2014. Dynamic modelling and optimisation of flexible operation in post-combustion CO_2 capture plants—A review. Comput. Chem. Eng. 61, 245–265.

Bui, M., Tait, P., Lucquiaud, M., Mac Dowell, N., 2018. Dynamic operation and modelling of amine-based CO_2 capture at pilot scale. Int. J. Greenh. Gas Control 79, 134–153.

Canepa, R., Wang, M., Biliyok, C., Satta, A., 2013. Thermodynamic analysis of combined cycle gas turbine power plant with post-combustion CO_2 capture and exhaust gas recirculation. Proc. Inst. Mech. Eng. Part E J. Process Mech. Eng. 227, 89–105.

Chen, C. -C, Evans, L.B., 1986. A local composition model for the excess Gibbs energy of

674 aqueous electrolyte systems. AIChE J. 32, 444–454.
675 Chilton, T.H., Colburn, A.P., 1934. Mass Transfer Coefficients: Prediction from Data on Heat
676 Transfer and Fluid Friction. Ind. Eng. Chem. 26, 1183–1187.
677 Coulson, J.M., Richardson, J.F., 2002. Chemical Engineering, 5th ed. Butterwoth Heinemann,
678 Oxford.
679 Dugas, R., 2006. Pilot Plant Study of Carbon Dioxide Capture by Aqueous Monoethanolamine.
680 MSE Thesis. University of Texas at Austin.
681 Dutta, R., Nord, L.O., Bolland, O., 2017. Selection and design of post-combustion CO_2 capture
682 process for 600 MW natural gas fueled thermal power plant based on operability. Energy
683 121, 643–656.
684 Eckert, J.S., 1970. Selecting the Proper Distillation Column Packing. Chem. Eng. Prog. 66,
685 39–44.
686 Enaasen, F.N., Knuutila, H., Kvamsdal, H.M., Hillestad, M., 2015. Dynamic model validation
687 of the post-combustion CO_2 absorption process. Int. J. Greenh. Gas Control 41, 127–141.
688 Enaasen, N.F., 2015. Post-combustion absorption-based CO_2 capture : modeling, validation
689 and analysis of process dynamics. PhD Thesis. Norwegian University of Science and
690 Technology.
691 Environmental Protection Agency, 2017. Global Greenhouse Gas Emissions Data. Available
692 at https://www.epa.gov/ghgemissions/global-greenhouse-gas-emissions-data%0D
693 (accessed on 20 March 2019).
694 Errico, M., Madeddu, C., Pinna, D., Baratti, R., 2016. Model calibration for the carbon dioxide-
695 amine absorption system. Appl. Energy 183, 958–968.
696 Fu, K., Chen, G., Liang, Z., Sema, T., Idem, R., 2014. Analysis of Mass Transfer Performance
697 of Monoethanolamine-Based CO_2 Absorption in a Packed Column Using Artificial Neural
698 Networks.
699 Garcia, M., Knuutila, H.K., Gu, S., 2017. Aspen Plus simulation model for CO_2 removal with
700 MEA: Validation of desorption model with experimental data. J. Environ. Chem. Eng. 5,
701 4693–4701.
702 Gaspar, J., Cormos, A.M., 2012. Dynamic modeling and absorption capacity assessment of
703 CO_2 capture process. Int. J. Greenh. Gas Control 8, 45–55.
704 Geankoplis, C.J., 2014. Transport Process & Separation Process Principles (Includes Unit
705 Operations), 4th ed. Pearson Education Limited, Essex.
706 Greer, T., Bedelbayev, A., Igreja, J.M., Gomes, J.F., Lie, B., 2010. A simulation study on the
707 abatement of CO_2 emissions by de-absorption with monoethanolamine. Environ. Technol.

708 31, 107–115.
709 Harun, N., Nittaya, T., Douglas, P.L., Croiset, E., Ricardez-Sandoval, L.A., 2012. Dynamic
710 simulation of MEA absorption process for CO_2 capture from power plants. Int. J. Greenh.
711 Gas Control 10, 295–309.
712 IEA-GHG, 2006. CO_2 capture in low rank coal power plant. IEA Greenh. Gas R&D Program.
713 Rep. no2006/1.
714 Khan, F.M., Krishnamoorthi, V., Mahmud, T., 2011. Modelling reactive absorption of CO_2 in
715 packed columns for post-combustion carbon capture applications. Chem. Eng. Res. Des.
716 89, 1600–1608.
717 Kister, H.Z., Gill, D.R., 1992. Flooding and Pressure Drop Prediction for Structured Packings.
718 IChemE Symp. Ser. 128 A109–A123.
719 Kister, H.Z., Gill, R.D., 1991. Predict Flood Point and Pressure Drop for Modern Random
720 Packings. Chem. Eng. Prog. 87, 32–42.
721 Kister, H.Z., Scherffius, J., Afshar, K., Abkar, E., 2007. Realistically predict capacity and
722 pressure drop for packed columns. Chem. Eng. Prog. 103, 28–38.
723 Kvamsdal, H.M., Jakobsen, J.P., Hoff, K.A., 2009. Dynamic modeling and simulation of a CO_2
724 absorber column for post-combustion CO_2 capture. Chem. Eng. Process. Process Intensif.
725 48, 135–144.
726 Lawal, A., Wang, M., Stephenson, P., Koumpouras, G., Yeung, H., 2010. Dynamic modelling
727 and analysis of post-combustion CO_2 chemical absorption process for coal-fired power
728 plants. Fuel 89, 2791–2801.
729 Lawal, A., Wang, M., Stephenson, P., Obi, O., 2012. Demonstrating full-scale post-combustion
730 CO_2 capture for coal-fired power plants through dynamic modelling and simulation. Fuel
731 101, 115–128.
732 Lawal, A., Wang, M., Stephenson, P., Yeung, H., 2009. Dynamic modelling of CO_2 absorption
733 for post combustion capture in coal-fired power plants. Fuel 88, 2455–2462.
734 Lemaire, E., Bouillon, P.A., Lettat, K., 2014. Development of HiCapt+ TM Process for CO_2
735 Capture from Lab to Industrial Pilot Plant. Oil Gas Sci. Technol. – Rev. d'IFP Energies
736 Nouv. 69, 1069–1080.
737 Leva, M., 1954. Flow Through Irrigated Dumped Packings. Chem. Eng. Prog. 50, 51–59.
738 Liu, Y., Hseuh, B.F., Gao, Z., Wong, D.S.H., Yao, Y., 2019. Dynamic Profile Monitoring for
739 Flooding Prognosis in Packed Columns. Chem. Eng. Technol. 42, 1232–1239.
740 Lobo, W.., Friend, L., Hashmall, H., Zenz, F.A., 1945. Limiting Capacity of Dumped Tower
741 Packings. Trans Am. Inst. Chem. Eng. 41, 693–710.

Luo, X., Wang, M., 2017. Improving Prediction Accuracy of a Rate-Based Model of an MEA-Based Carbon Capture Process for Large-Scale Commercial Deployment. Engineering 3, 232–243.

Marx-Schubach, T., Schmitz, G., 2019. Modeling and simulation of the start-up process of coal fired power plants with post-combustion CO_2 capture. Int. J. Greenh. Gas Control 87, 44–57.

Nittaya, T., Douglas, P.L., Croiset, E., Ricardez-Sandoval, L.A., 2014. Dynamic modeling and evaluation of an industrial-scale CO_2 capture plant using monoethanolamine absorption processes. Ind. Eng. Chem. Res. 53, 11411–11426.

Onda, K., Takeuchi, H., Okumoto, Y., 1968. Mass transfer coefficients between gas and liquid phases in packed columns. J. Chem. Eng. Japan 1, 56–62.

Piché, S., Larachi, F., Grandjean, B.P.A., 2001. Loading capacity in packed towers - Database, correlations and analysis. Chem. Eng. Technol. 24, 373–380.

Pintola, T., Tontiwachwuthikul, P., Meisen, A., 1993. Simulation of pilot plant and industrial CO_2-MEA absorbers. Gas Sep. Purif. 7, 47–52.

Plaza, J.M., Rochelle, G.T., 2011. Modeling pilot plant results for CO_2 capture by aqueous piperazine. Energy Procedia 4, 1593–1600.

Razi, N., Svendsen, H.F., Bolland, O., 2013. Validation of mass transfer correlations for CO_2 absorption with MEA using pilot data. Int. J. Greenh. Gas Control 19, 478–491.

Reddy, S., Johnson, D., Gilmartin, J., 2008. Fluor's econamine FG plus^{SM} technology for CO_2 capture at coal-fired power plants. Air Waste Manag. Assoc. - 7th Power Plant Air Pollut. Control "Mega" Symp. 2008 1, 63–79.

Reddy, S., Scherffius, J.R., Yonkoski, J., Radgen, P., Rode, H., 2013. Initial results from fluor's CO_2 capture demonstration plant using econamine FG PlusSM technology at E.ON Kraftwerke's wilhelmshaven power plant. Energy Procedia 37, 6216–6225.

Rezazadeh, F., Gale, W.F., Rochelle, G.T., Sachde, D., 2017. Effectiveness of absorber intercooling for CO_2 absorption from natural gas fired flue gases using monoethanolamine solvent. Int. J. Greenh. Gas Control 58, 246–255.

Scherffius, J.R., Reddy, S., Klumpyan, J.P., Armpriester, A., 2013. Large-scale CO_2 capture demonstration plant using fluor's econamine FG Plus^{SM} technology at NRG's WA parish electric generating station. Energy Procedia 37, 6553–6561.

Seader, J.D., Seider, W.D., Lewin, D.R., Boulle, L., Rycrof, A., 2006. Separation Process Principles, 3rd ed. John Wiley & Sons, INC, Hoboken, NJ.

Sherwood, T.K., Shipley, G.H., Holloway, F.A.L., 1938. Flooding Velocities in Packed

776 Columns. Ind. Eng. Chem. 30, 765–769.
777 Sinnott, R.K., 2005. Chemical Engineering Design, Fouth Edit. Coulson & Richardson's
778 Chemical Engineering series. Elsevier Butterworth-Heinemann, Oxford.
779 Soave, G., 1972. Equilibrium constants from a modified Redlich-Kwong equation of state.
780 Chem. Eng. Sci. 27, 1197–1203.
781 Soltani, S.M., Fennell, P.S., Mac Dowell, N., 2017. A parametric study of CO_2 capture from
782 gas-fired power plants using monoethanolamine (MEA). Int. J. Greenh. Gas Control 63,
783 321–328.
784 Sreedhar, I., Nahar, T., Venugopal, A., Srinivas, B., 2017. Carbon capture by absorption – Path
785 covered and ahead. Renew. Sustain. Energy Rev. 76, 1080–1107.
786 Stichlmair, J., Bravo, J.L., Fair, J.R., 1989. General model for prediction of pressure drop anc
787 capacity of countercurrent gas/liquid packed column. Gas Sep. Purif. 61, 19–28.
788 Strigle, R.F., 1994. Packed tower design and applications: random and structured packings,
789 2nd ed. Gulf Publishing Company, Houston.
790 Tontiwachwuthikul, P., Meisen, A., Lim, C.J., 1992. CO_2 absorption by NaOH,
791 monoethanolamine and 2-amino-2-methyl-1-propanol solutions in a packed column.
792 Chem. Eng. Sci. 47, 381–390.
793 Wang, M., Lawal, A., Stephenson, P., Sidders, J., Ramshaw, C., 2011. Post-combustion CO_2
794 capture with chemical absorption: A state-of-the-art review. Chem. Eng. Res. Des. 89,
795 1609–1624.
796 Warudkar, S.S., Cox, K.R., Wong, M.S., Hirasaki, G.J., 2013. Influence of stripper operating
797 parameters on the performance of amine absorption systems for post-combustion carbon
798 capture: Part I. High pressure strippers. Int. J. Greenh. Gas Control 16, 342–350.
799 Wolf-Zöllner, V., Seibert, F., Lehner, M., 2019a. Extended performance comparison of
800 different pressure drop, hold-up and flooding point correlations for packed columns.
801 Chem. Eng. Res. Des. 147, 699–708.
802 Zhang, Y., Chen, C.C., 2013. Modeling CO_2 absorption and desorption by aqueous
803 monoethanolamine solution with Aspen rate-based model. Energy Procedia 37, 1584–
804 1596.
805 Zhang, Y., Chen, H., Chen, C.C., Plaza, J.M., Dugas, R., Rochelle, G.T., 2009. Rate-based
806 process modeling study of CO_2 Capture with aqueous monoethanolamine solution. Ind.
807 Eng. Chem. Res. 48, 9233–9246.
808 Ziaii, S., Rochelle, G.T., Edgar, T.F., 2009. Dynamic modeling to minimize energy use for

809 CO_2 capture in power plants by aqueous monoethanolamine. Ind. Eng. Chem. Res. 48, 6105–
810 6111.